Supporting Information

Oxygen Defect-mediated $NiCo_2O_4$ Nanosheets as Electrode for Pseudocapacitor with Improved Rate Capability

Wen You[a#], Mengyuan Li[b#], Qiong Li[b], Jizhou Jiang[b], Kun Xiang[b,c,*], Mingjiang Xie[d,*]

[a] Editorial Department of Journal of Wuhan Institute of Technology, Wuhan Institute of Technology, Wuhan 430205, China

[b] School of Chemistry and Environmental Engineering, School of Environmental Ecology and Biological Engineering, Engineering Research Center of Phosphorus Resources Development and Utilization of Ministry of Education, Wuhan Institute of Technology, Wuhan 430205, China

[c] Key Laboratory of Optoelectronic Chemical Materials and Devices of Ministry of Education, Jianghan University, Wuhan 430205, China

[d] Hubei Key Laboratory for Processing and Application of Catalytic Materials, Huanggang Normal University, Huanggang 438000, China

[#] W. You and M. Y. Li contributed equally to this work.

Experimental Section

Synthesis of r-$NiCo_2O_4$ nanosheets: In a typical synthesis, 1.1 mmol $Ni(NO_3)_2$•$6H_2O$, 2.2 mmol $Co(NO_3)_2$•$6H_2O$ and 13.2 mmol hexamethylenetetramine (HMT) are dissolved into 80 mL mixed solution of ethylene glycol/water (v/v=7/1) to form the clear pink solution after violent stirring for 30 min. Then the clear pink solution is transferred into a 100 mL Teflon lined stainless autoclave. The autoclave is sealed and maintained at 120°C for 4 hours and then cooled down to room temperature. The precipitates are collected by centrifugation and rinsed for three times with abundant amount of deionized water and ethanol, respectively. Then, the green solid product is dried at –40°C in freezing dryer for 36 h. The dried samples are further calcined at 300°C for 2 hours in the air to convert the hydroxide into the $NiCo_2O_4$. For oxygen defect-mediated $NiCo_2O_4$, 0.1 g original $NiCo_2O_4$ NSs are immersed in 100 mL 1.0 M $NaBH_4$ solution for 1 h at room temperature. After reduction, the samples are filtered, thoroughly washed with deionized water and ethanol for several times and dried in a vacuum oven at 60°C for 12 h. The synthesis process of the irregular $NiCo_2O_4$ NPs is similar to the aforementioned method, while the solvent is all deionized water and the reaction time is 12 hours.

Characterization: The samples are characterized by field emission scanning electron microscopy (FESEM, Hitachi, S-4800), transmission electron microscopy (TEM, JEOL, JEM-1101), high-resolution transmission electron microscopy (HRTEM, JEOL, JEM-2100) and X-ray powder diffractometry

(XRD, Bruker D8 Advance X-ray diffractometer system with Co Kα radiation of 1.7902 Å.). The specific surface areas of the products are evaluated by the ASAP 2020 instrument. An X-ray photoelectron spectroscopy (XPS) survey is conducted using a PHI 5000 VersaProbe with an Al Kα excitation source. The Raman spectra are obtained using a Renishaw in Via Reflex Raman system with the excitation laser of 532 nm. The electrical conductivity is measured by a four-wire method using a source measure unit (SMU, Keithley 6430). Thermal gravimetry analysis (TGA) is recorded on Netzsch STA 449C under air and nitrogen atmosphere with the heating rate of 5 ^{o}C/min.

Electrochemical Measurements: The working electrode is prepared by mixing 80 wt.% as-made products, 10 wt.% acetylene black, and 10 wt.% polytetrafluoroethylene (PTFE) in small amount of ethanol to obtain the slurry mixture. The obtained slurry is coated on the single surface of nickel foams with a size of 1 cm × 1 cm and dried in vacuum at 80°C for 12 h. Then, the nickel foams with the electroactive materials are pressed under 10 MPa with the thickness of 0.11 mm. The mass loading of active material is about 1.8 mg cm^{-2}. The electrochemical tests of all samples are conducted in a three-electrode system with a Pt counter-electrode and an Hg/HgO reference electrode in 6.0 M KOH solution. The electrochemical AC impedance measurements are carried out to assess the electrical properties at an open circuit voltage with frequency from 0.01 Hz to 100 kHz and an amplitude of 5 mV. All the electrochemical tests are carried out on the electrochemical working station (CHI660E, Shanghai, China).

The specific capacitance of the supercapacitor can be calculated by galvanostatic discharge-charge (GCD) test as following equation:

$$C_m = \frac{I}{m} \times \frac{\Delta t}{\Delta V}$$

Where C_m is the specific capacitance of the capacitor (F g^{-1}); I is the current of the charge/discharge process; Δt is the discharging time period in seconds for the potential change ΔV, in volts; m is the mass loading of the active material. All the electrochemical measurements are carried out at room temperature.

Supplementary Figures and Tables

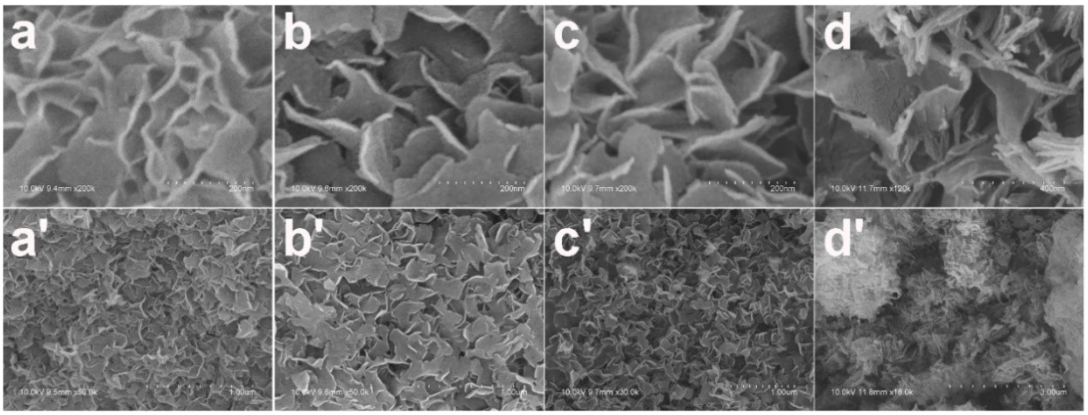

Figure S1. SEM images of nickel-cobalt hydroxides nanosheets obtained at various solvothermal reaction times: (a) and (a') for 1 h; (b) and (b') for 2 h; (c) and (c') for 4 h; (d) and (d') for 6 h.

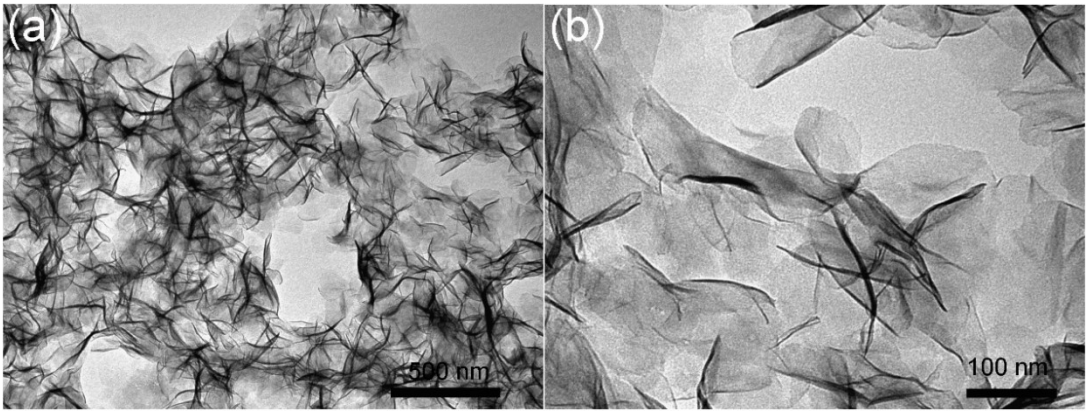

Figure S2. TEM images of optimized nickel-cobalt hydroxide nanosheets at 120 °C for 4 h.

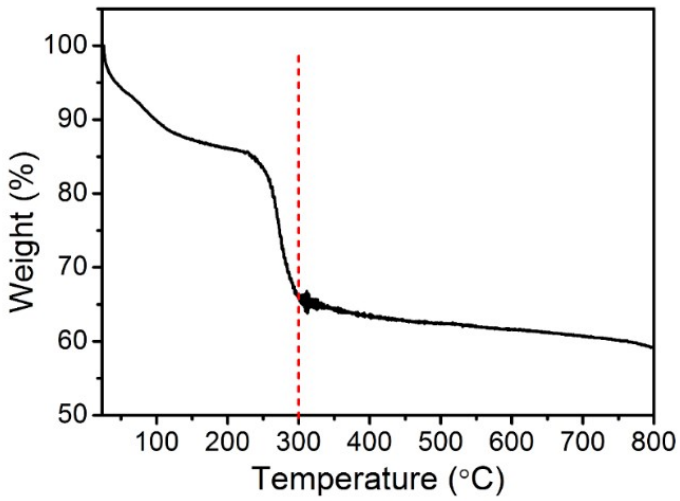

Figure S3. TGA curve of optimized nickel-cobalt hydroxide nanosheets at 120 °C for 4 h.

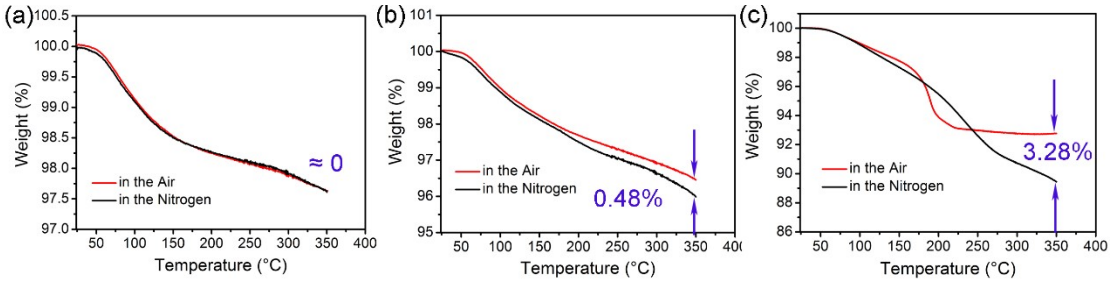

Figure S4. TGA analysis of (a) $NiCo_2O_4$ NPs, (b) original $NiCo_2O_4$ NSs and (c) r-$NiCo_2O_4$ NSs in air and argon atmosphere. (Flow of 20 mL min^{-1} and a ramping rate of 5°C/min). The concentrations of oxygen defects are calculated from the difference in weight decrease between the two TGA curves.

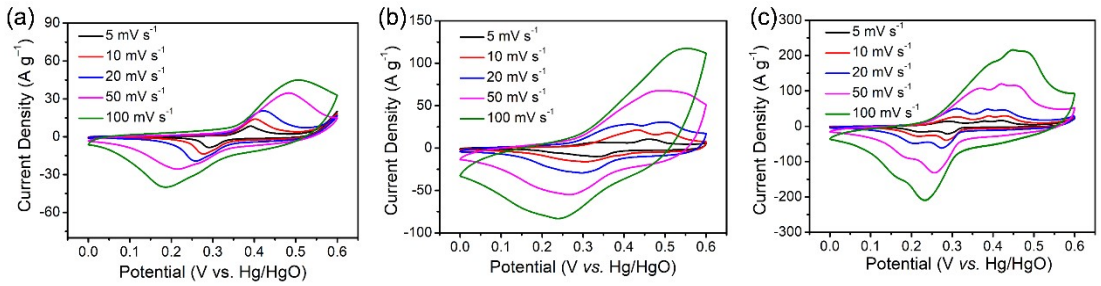

Figure S5. CV curves of $NiCo_2O_4$ NPs, original $NiCo_2O_4$ and r-$NiCo_2O_4$ NSs at various scan rates.

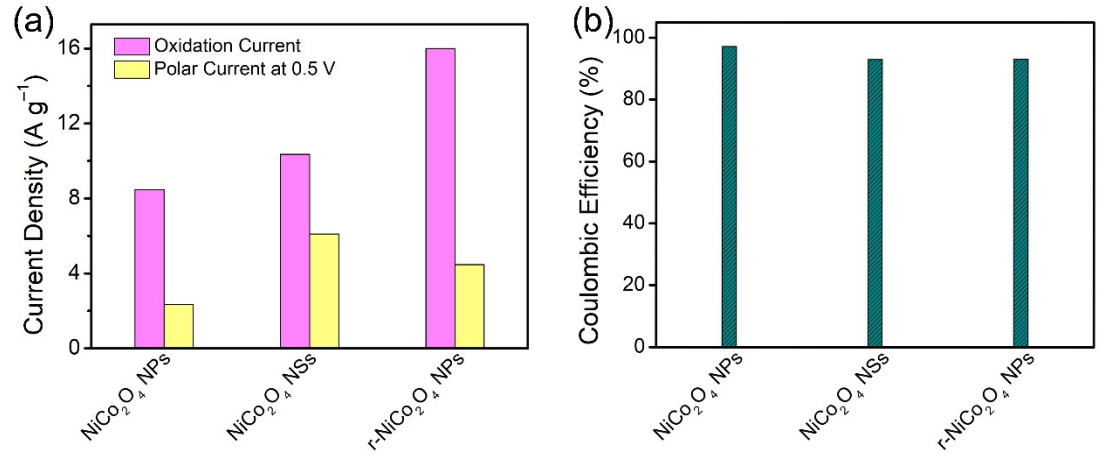

Figure S6. (a) The polarization currents at 0.5 V and the oxidation currents of $NiCo_2O_4$ NPs, $NiCo_2O_4$ NSs, and r-$NiCo_2O_4$ NSs electrodes. (b) Coulombic efficiencies of $NiCo_2O_4$ NPs, $NiCo_2O_4$ NSs, and r-$NiCo_2O_4$ NSs at the current density of 20 A g^{-1}.

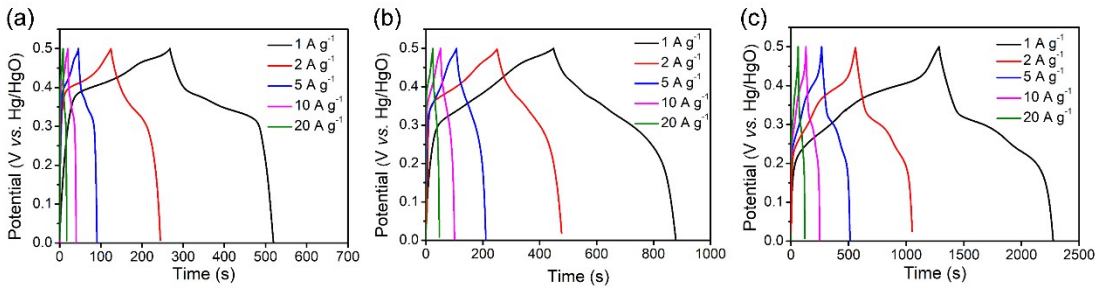

Figure S7. (a-c) Galvanostatic charge and discharge voltage profiles of $NiCo_2O_4$ NPs, original $NiCo_2O_4$ and r-$NiCo_2O_4$ NSs at various current densities.

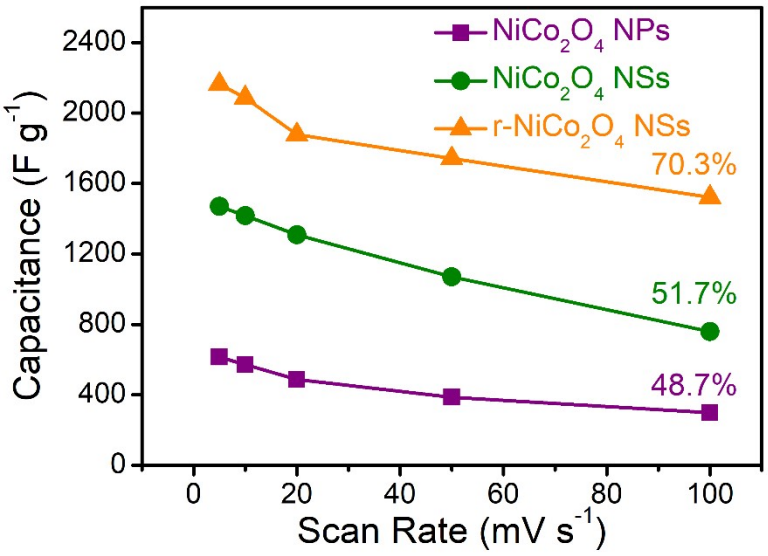

Figure S8. Plots of specific capacitance as a function of scan rate of $NiCo_2O_4$ NPs, original $NiCo_2O_4$ NSs, and r-$NiCo_2O_4$ NSs.

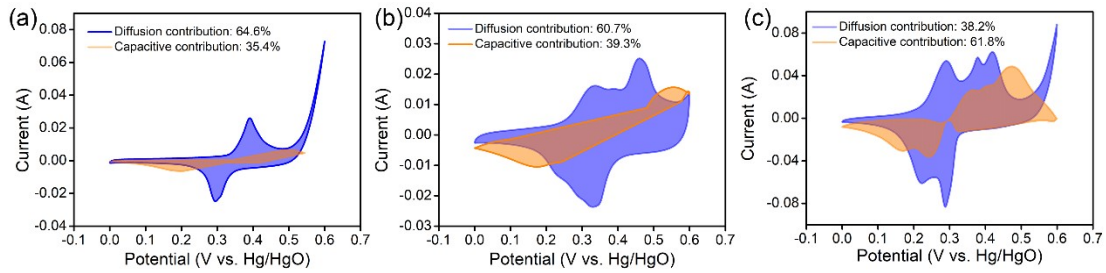

Figure S9. Diffusion and capacitive-controlled current contributions of $NiCo_2O_4$ NPs, original $NiCo_2O_4$ NSs, and r-$NiCo_2O_4$ NSs calculated from CV curves at the scan rate of 5 mV s^{-1}.

Table S1. Comparison of the electrochemical performances of r-$NiCo_2O_4$ electrode in this work with $NiCo_2O_4$ and carbon-based electrodes in the literature

$NiCo_2O_4$-based electrode	Specific capacitance		Rate capability	Ref.
	C_{min}	C_{max}		
Mesoporous $NiCo_2O_4$	956 F g^{-1} @ 1 A g^{-1}	828 F g^{-1} @ 10 A g^{-1}	86.6% (1-10 A g^{-1})	1
rGO wrapped porous $NiCo_2O_4$	1176 F g^{-1} @ 2 A g^{-1}	1020 F g^{-1} @ 8 A g^{-1}	86.7% (2-8 A g^{-1})	2
$NiCo_2O_4$-decorated porous carbon	596.8 F g^{-1} @ 2 A g^{-1}	185 F g^{-1} @ 20 A g^{-1}	30.9% (2-20 A g^{-1})	3
$NiCo_2O_4$ tetragonal microtubes	1388 F g^{-1} @ 2 A g^{-1}	863 F g^{-1} @ 30 A g^{-1}	62.2% (2-30 A g^{-1})	4
nickel cobalt oxide/graphene oxide	1211 F g^{-1} @ 1 A g^{-1}	687 F g^{-1} @ 10 A g^{-1}	56.7% (1-10 A g^{-1})	5
$NiCo_2O_4$ hollow spheres	1204 F g^{-1} @ 2 A g^{-1}	822 F g^{-1} @ 20 A g^{-1}	68.3% (1-20 A g^{-1})	6
$NiCo_2O_4$ microspheres	1822.3 F g^{-1} @ 2 A g^{-1}	1250.9 F g^{-1} @ 20 A g^{-1}	68.6% (1-20 A g^{-1})	7
Ni/Co porous oxide nanosheets	830 F g^{-1} @ 1 A g^{-1}	710 F g^{-1} @ 20 A g^{-1}	85.5% (1-20 A g^{-1})	8
Mesoporous $NiCo_2O_4$	655 F g^{-1} @ 1 A g^{-1}	430 F g^{-1} @ 10 A g^{-1}	65.6% (1-10 A g^{-1})	9
hollow $NiCo_2O_4$ nanospheres	1229 F g^{-1} @ 1 A g^{-1}	1027 F g^{-1} @ 25 A g^{-1}	83.6% (1-25 A g^{-1})	10
Mesoporous $NiCo_2O_4$/NF	708 F g^{-1} @ 1 A g^{-1}	628 F g^{-1} @ 10 A g^{-1}	88.7% (1-10 A g^{-1})	11
N-doped graphene framework (NCO/NGF)	1198 F g^{-1} @ 1 A g^{-1}	634 F g^{-1} @ 20 A g^{-1}	52.9% (1-20 A g^{-1})	12
rGO/$NiCo_2O_4$	1003 F g^{-1} @ 1 A g^{-1}	893 F g^{-1} @ 10 A g^{-1}	89.0% (1-10 A g^{-1})	13
$NiCo_2O_4$/CuO-x	1670 F g^{-1} @ 1 A g^{-1}	692 F g^{-1} @ 10 A g^{-1}	41.4% (1-10 A g^{-1})	14
rHGO/ $NiCo_2O_4$@CF	1178 F g^{-1} @ 1 A g^{-1}	1100.4 F g^{-1} @ 10 A g^{-1}	93.4% (1-10 A g^{-1})	15

Co–Ni–O/3DG	1586 F g^{-1} @ 1 A g^{-1}	~ 1100 F g^{-1} @ 10 A g^{-1}	69.4% (1-10 A g^{-1})	16
$NiCo_2O_4$@GQDs	1382 F g^{-1} @ 1 A g^{-1}	1278 F g^{-1} @ 20 A g^{-1}	92.5% (1-20 A g^{-1})	17
hexagonal $NiCo_2O_4$	1525 F g^{-1} @ 1 A g^{-1}	610 F g^{-1} @ 10 A g^{-1}	40.0% (1-10 A g^{-1})	18
$NiCo_2O_4$ Nanoparticle	1084 F g^{-1} @ 2 A g^{-1}	300 F g^{-1} @ 10 A g^{-1}	27.7% (2-10 A g^{-1})	19
P- $NiCo_2O_4$	1642 F g^{-1} @ 2 A g^{-1}	1335 F g^{-1} @ 20 A g^{-1}	81.3% (2-20 A g^{-1})	20
$NiCo_2O_4$@AMCRs	1691 F g^{-1} @ 3 A g^{-1}	1275 F g^{-1} @ 20 A g^{-1}	75.4% (3-20 A g^{-1})	21
$NiCo_2O_4$/PANI/MF	1540.1 F g^{-1} @ 1 A g^{-1}	1220 F g^{-1} @ 20 A g^{-1}	79.2% (1-20 A g^{-1})	22
Mesoporous $NiCo_2O_4$ flower	122.5 C g^{-1} @ 1 A g^{-1}	82.5 C g^{-1} @ 10 A g^{-1}	67.3% (1-10 A g^{-1})	23
$NiCo_2O_4$/carbon	1480.9 F g^{-1} @ 1 A g^{-1}	995.2 F g^{-1} @ 20 A g^{-1}	67.2% (1-20 A g^{-1})	24
$NiCo_2O_4$/Carbonized melamine foam	1541 F g^{-1} @ 1 A g^{-1}	1120 F g^{-1} @ 20 A g^{-1}	72.7% (1-20 A g^{-1})	25
Hierarchically porous carbon	218.6 F g^{-1} @ 1 A g^{-1}	164.5 F g^{-1} @ 20 A g^{-1}	75.3% (1-20 A g^{-1})	26
O-N-S co-doped hierarchical porous carbon	576 F g^{-1} @ 1 A g^{-1}	267 F g^{-1} @ 20 A g^{-1}	43.4% (1-20 A g^{-1})	27
Porous carbon sheets	407 F g^{-1} @ 1 A g^{-1}	224 F g^{-1} @ 20 A g^{-1}	55.0% (1-20 A g^{-1})	28
Carbon spheres@ porous carbon	337 F g^{-1} @ 1 A g^{-1}	280 F g^{-1} @ 20 A g^{-1}	83.1% (1-20 A g^{-1})	29
N-doped porous graphene	390 F g^{-1} @ 1 A g^{-1}	238 F g^{-1} @ 20 A g^{-1}	61.0% (1-20 A g^{-1})	30
Ultrathin $NiCo_2O_4$ Nanosheets/NF	2010 F g^{-1} @ 2 A g^{-1}	1450 F g^{-1} @ 20 A g^{-1}	72.1% (2-20 A g^{-1})	31
Ultrathin $NiCo_2O_4$ Nanosheets/CF	1002 F g^{-1} @ 1 A g^{-1}	520 F g^{-1} @ 1 A g^{-1}	48.8% (1-20 A g^{-1})	32
Porous $NiCo_2O_4$ Nanosheet/Carbon Fabric	2658 F g^{-1} @ 2 A g^{-1}	1866 F g^{-1} @ 20 A g^{-1}	70.2% (2-20 A g^{-1})	33
Pd-$NiCo_2O_4$ /NF	2484.4 F g^{-1} @ 2 A g^{-1}	2011 F g^{-1} @ 2 A g^{-1}	80.9% (2-20 A g^{-1})	34
Mesoporous $NiCo_2O_4$ Nanosheets	560 F g^{-1} @ 2 A g^{-1}	400 F g^{-1} @ 2 A g^{-1}	71.4% (2-20 A g^{-1})	35
r-$NiCo_2O_4$ nanosheets	**1980 F g^{-1} @ 1 A g^{-1}** **1968 F g^{-1} @ 2 A g^{-1}**	**1897 F g^{-1} @ 10 A g^{-1}** **1812 F g^{-1} @ 20A g^{-1}**	**95.8% (1-10 A g^{-1})** **91.5% (1-20 A g^{-1})**	**This work**

			92/1% (2-20 A g^{-1})	

Reference

[1] Y. Liu, Z. Wang, Y. Zhong, M. Tade, W. Zhou, Z. Shao, Molecular Design of Mesoporous $NiCo_2O_4$ and $NiCo_2S_4$ with Sub-Micrometer-Polyhedron Architectures for Efficient Pseudocapacitive Energy Storage. Adv. Funct. Mater., 27 (2017) 1701229.

[2] S. Al-Rubaye, R. Rajagopalan, S. X. Dou, Z. Cheng, Facile synthesis of a reduced graphene oxide wrapped porous $NiCo_2O_4$ composite with superior performance as an electrode material for supercapacitors. J. Mater. Chem. A, 5 (2017) 18989.

[3] V. Veeramani, R. Madhu, S.-M. Chen, M. Sivakumar, C.-T. Hung, N. Miyamoto, S.-B. Liu, $NiCo_2O_4$-decorated porous carbon nanosheets for high-performance supercapacitors. Electrochim. Acta 247 (2017) 288.

[4] F.-X. Ma, L. Yu, C.-Y. Xu, X. W. Lou, Self-supported formation of hierarchical $NiCo_2O_4$ tetragonal microtubes with enhanced electrochemical properties. Energy Environm. Sci., 9 (2016) 862.

[5] Y. Xu, L. Wang, P. Cao, C. Cai, Y. Fu, X. Ma, Mesoporous composite nickel cobalt oxide/graphene oxide synthesized via a template-assistant co-precipitation route as electrode material for supercapacitors. J. Power Sources, 306 (2016) 742.

[6] J. Guo, Z. Yin, X. Zang, Z. Dai, Y. Zhang, W. Huang, X. Dong, Facile one-pot synthesis of $NiCo_2O_4$ hollow spheres with controllable number of shells for high-performance supercapacitors. Nano Res., 10 (2017) 405.

[7] M. Cheng, H. Fan, Y. Song, Y. Cui, R. Wang, Interconnected hierarchical $NiCo_2O_4$ microspheres as high-performance electrode materials for supercapacitors. Dalton Trans., 46 (2017) 9201.

[8] S. Jiang, Y. Sun, Z. Li, X. Zeng, H. Yang, Facile Synthesis of Porous $NiCoO_2$ Nanosheets as Ultra-High Rate Redox-Capacitive Materials. J. Electrochem. Soc., 164 (2017) A1158.

[9] L. Zhang, D. Zhang, Z. Ren, M. Huo, G. Dang, F. Min, Q. Zhang, J. Xie, Mesoporous $NiCo_2O_4$ Micro/nanospheres with Hierarchical Structures for Supercapacitors and Methanol Electro-oxidation. ChemElectroChem 4 (2017) 441.

[10] K. Xu, J. Yang, J. Hu, Synthesis of hollow $NiCo_2O_4$ nanospheres with large specific surface area for asymmetric supercapacitors. J. Colloid Interf. Sci., 511 (2018) 456.

[11] J. Q. Qi, S. L. Li, Y. W. Sui, Y. Z. He, Q. K. Meng, F. X. Wei, Y. J. Ren, Y. X. Jin, Solvent dependence on structure and supercapacitor performance of mesoporous $NiCo_2O_4$ grown on nickel foam. Mater. Res. Express, 4 (2017) 106302.
[12] Y. Chen, T. Liu, L. Zhang, J. Yu, N-doped graphene framework supported nickel cobalt oxide as supercapacitor electrode with enhanced performance. Appl. Surf. Sci., 484 (2019) 135.
[13] S. Zhang, H. Gao, J. Zhou, F. Jiang, Z. Zhang, Hydrothermal synthesis of reduced graphene oxide-modified $NiCo_2O_4$ nanowire arrays with enhanced reactivity for supercapacitors. J. Alloys Comp., 792 (2019) 474.
[14] Y. Zhang, Y. Ru, S.-W. Wang, H.-L. Gao, J. Yan, H.-W. Luo, K.-Z. Gao, H. Fang, A.-q. Zhang, L.-Z. Wang, X.-D. Jia, Facilely synthesized $NiCo_2O_4$/CuO-x composite with improved electrochemical behavior for high-rate supercapacitors. Mater. Res. Express, 6 (2019) 075518.
[15] S. Li, K. Yang, P. Ye, H. Jiang, Z. Zhang, Q. Huang, L. Wang, Hierarchical interpenetrating rHGO-decorated $NiCo_2O_4$ nanowires architectures for high-performance supercapacitors. Appl. Surf. Sci., 473 (2019) 326.
[16] C. Xiang, Y. Liu, Y. Yin, P. Huang, Y. Zou, M. Fehse, Z. She, F. Xu, D. Banerjee, D. Hermida Merino, A. Longo, H.-B. Kraatz, D. F. Brougham, B. Wu, L. Sun, Facile Green Route to Ni/Co Oxide Nanoparticle Embedded 3D Graphitic Carbon Nanosheets for High Performance Hybrid Supercapacitor Devices. ACS Appl. Energy Mater., 2 (2019) 3389.
[17] J. Luo, J. Wang, S. Liu, W. Wu, T. Jia, Z. Yang, S. Mu, Y. Huang, Graphene quantum dots encapsulated tremella-like $NiCo_2O_4$ for advanced asymmetric supercapacitors. Carbon, 146 (2019) 1.
[18] J. Bhagwan, G. Nagaraju, B. Ramulu, S. C. Sekhar, J. S. Yu, Rapid synthesis of hexagonal $NiCo_2O_4$ nanostructures for high-performance asymmetric supercapacitors. Electrochim. Acta, 299 (2019) 509.
[19] L. Kumar, H. Chauhan, N. Yadav, N. Yadav, S. A. Hashmi, S. Deka, Faster Ion Switching $NiCo_2O_4$ Nanoparticle Electrode-Based Supercapacitor Device with High Performances and Long Cycling Stability. ACS Appl. Energy Mater., 1 (2018) 6999.
[20] W. Qiu, H. Xiao, M. Yu, Y. Li, X. Lu, Surface modulation of $NiCo_2O_4$ nanowire arrays with significantly enhanced reactivity for ultrahigh-energy supercapacitors. Chem. Eng. J., 352 (2018) 996.
[21] Y. Pang, S. Zhang, S. Chen, J. Liang, M. Li, D. Ding, S. Ding, Transition-Metal Oxides Anchored on Nitrogen-Enriched Carbon Ribbons for High-Performance Pseudocapacitors. Chem. Eur. J., 24 (2018) 16104.
[22] F. Cui, Y. Huang, L. Xu, Y. Zhao, J. Lian, J. Bao, H. Li, Rational construction of a 3D hierarchical $NiCo_2O_4$/PANI/MF composite foam as a high-performance electrode for asymmetric supercapacitors. Chem. Commun., 54 (2018) 4160.
[23] W. Jiang, F. Hu, Q. Yan, X. Wu, Investigation on electrochemical behaviors of $NiCo_2O_4$ battery-type supercapacitor electrodes: the role of

an aqueous electrolyte. Inorg. Chem. Front., 4 (2017) 1642.
[24] G. Yang, S.-J. Park, Facile hydrothermal synthesis of $NiCo_2O_4$-decorated filter carbon as electrodes for high performance asymmetric supercapacitors. Electrochim. Acta, 285 (2018) 405.
[25] Z. Qu, M. Shi, H. Wu, Y. Liu, J. Jiang, C. Yan, An efficient binder-free electrode with multiple carbonized channels wrapped by $NiCo_2O_4$ nanosheets for high-performance capacitive energy storage. J. Power Sources, 410-411 (2019) 179.
[26] S. Luan, W. Li, X. Hou, Z. Guo, W. Li, Y. Song, X. Zhang, Q. Wang, CO_2-induced architectural transition of hierarchically porous carbon in reverse microemulsion system. Carbon, 151 (2019) 18.
[27] G. Zhao, C. Chen, D. Yu, L. Sun, C. Yang, H. Zhang, Y. Sun, F. Besenbacher, M. Yu, One-step production of O-N-S co-doped three-dimensional hierarchical porous carbons for high-performance supercapacitors. Nano Energy, 47 (2018) 547.
[28] C. Wang, D. Wu, H. Wang, Z. Gao, F. Xu, K. Jiang, A green and scalable route to yield porous carbon sheets from biomass for supercapacitors with high capacity. J. Mater. Chem. A, 6 (2018) 1244.
[29] S. Liu, Y. Zhao, B. Zhang, H. Xia, J. Zhou, W. Xie, H. Li, Nano-micro carbon spheres anchored on porous carbon derived from dual-biomass as high rate performance supercapacitor electrodes. J. Power Sources, 381 (2018) 116.
[30] S. Dai, Z. Liu, B. Zhao, J. Zeng, H. Hu, Q. Zhang, D. Chen, C. Qu, D. Dang, M. Liu, A high-performance supercapacitor electrode based on N-doped porous graphene. J. Power Sources, 387 (2018) 43.
[31] C. Yuan , J. Li , L. Hou , X. Zhang , L. Shen, X. Lou, Ultrathin Mesoporous $NiCo_2O_4$ Nanosheets Supported on Ni Foam as Advanced Electrodes for Supercapacitors. Adv. Funct. Mater., 22 (2012) 4592.
[32] G. Zhang, X. Lou, Controlled Growth of $NiCo_2O_4$ Nanorods and Ultrathin Nanosheets on Carbon Nanofibers for High-performance Supercapacitors. Sci. Rep., 3 (2013) 1470.
[33] J. Du, G. Zhou, H. Zhang, C. Cheng, J. Ma, W. Wei, L. Chen, T. Wang, Ultrathin Porous $NiCo_2O_4$ Nanosheet Arrays on Flexible Carbon Fabric for High-Performance Supercapacitors. ACS Appl. Mater. Interfaces, 5 (2013) 7405.
[34] H. Tong, Q. Meng, J. Liu, T. Li, D. Gong, J. Xiao, L. Shen, T. Zhang, D. Bing, X. Zhang, Cross-linked $NiCo_2O_4$ nanosheets with low crystallinity and rich oxygen vacancies for asymmetric supercapacitors. J. Alloys Compd., 822 (2020) 153689.
[35] A. K. Mondal, D. Su, S. Chen, K. Kretschmer, X. Xie, H.-J. Ahn, G. Wang, A Microwave Synthesis of Mesoporous $NiCo_2O_4$ Nanosheets as Electrode Materials for Lithium-Ion Batteries and Supercapacitors. ChemphysChem, 16 (2015) 169.